HHS Public Access

Author manuscript

J Control Release. Author manuscript; available in PMC 2022 May 04.

Published in final edited form as:

J Control Release. 2021 February 10; 330: 329–340. doi:10.1016/j.jconrel.2020.12.010.

Formulation and efficacy of ECO/*pRHO-ABCA4-SV40* nanoparticles for nonviral gene therapy of Stargardt disease in a mouse model

Da Sun[a,1], **Wenyu Sun**[a,1], **Song-Qi Gao**[a], **Cheng Wei**[a], **Amirreza Naderi**[a], **Andrew L. Schilb**[a], **Josef Scheidt**[a], **Sangjoon Lee**[a], **Timothy S. Kern**[b,c], **Krzysztof Palczewski**[b], **Zheng-Rong Lu**[a,*]

[a]Department of Biomedical Engineering, Case Western Reserve University, Cleveland, OH 44106, United States of America

[b]Department of Ophthalmology, Physiology & Biophysics, and Chemistry, University of California, Irvine, Irvine, CA 92697, United States of America

[c]Veterans Administration Medical Center Research Service, Long Beach, CA, 90822, United States of America

Abstract

It is still a challenge to develop gene replacement therapy for retinal disorders caused by mutations in large genes, such as Stargardt disease (STGD). STGD is caused by mutations in *ABCA4* gene. Previously, we have developed an effective non-viral gene therapy using self-assembled nanoparticles of a multifunctional pH-sensitive amino lipid ECO and a therapeutic *ABCA4* plasmid containing rhodopsin promoter (*pRHO–ABCA4*). In this study, we modified the *ABCA4* plasmid with simian virus 40 enhancer (*SV40, pRHO–ABCA4–SV40*) for enhanced gene expression. We also prepared and assessed the formulations of ECO/*pDNA* nanoparticles using sucrose or sorbitol as a stablilizer to develop consistent and stable formulations. Results demonstrated that ECO formed stable nanoparticles with *pRHO–ABCA4–SV40* in the presence of sucrose, but not with sorbitol. The transfection efficiency *in vitro* increased significantly after introduction of *SV40* enhancer for plasmid *pCMV-ABCA4–SV40* with a *CMV* promoter. Sucrose didn't affect the transfection efficiency, while sorbitol resulted in a fluctuation of the *in vitro* transfection efficiency. Subretinal gene therapy in *Abca4*$^{-/-}$ mice using ECO/*pRHO–ABCA4* and ECO/*pRHO–ABCA4–SV40* nanoparticles induced 36% and 29% reduction in A2E

*Corresponding author at: M. Frank Rudy and Margaret Domiter Rudy Professor of Biomedical Engineering, Department of Biomedical Engineering, Case Western Reserve University, Wickenden 427, Mail Stop 7207, 10900 Euclid Avenue, Cleveland, OH 44106, United States of America. zxl125@case.edu (Z.-R. Lu).

[1]These authors contribute equally to this work.

Author contributions

Z.R.L. and D.S. conceived the conceptualization of the project. D.S. and W.S. were involved in all aspects of this work including data curation, analysis, investigation, methodology, project administration and validation. S.Q.G performed HPLC analysis of the samples (data curation and analysis). C.W., A.N., A.L.S., and J.S. performed nanoparticle formulation, characterization, and qRT-PCR analysis (methodology, data curation and formal analysis). S.L. performed on cytotoxicity experiment and data analysis (methodology, data curation and formal analysis). T.K. and K.P. provided assistance with animal model resources and experiment design and conceptualization (conceptualization, resources). D.S. prepared the first draft (writing-original draft). D.S. and Z. R.L. revised and completed the final version (writing- review & editing). All authors read and approved the final paper.

Declaration of competing interest

The authors have declared that no conflict of interest exists.

accumulation respectively. Therefore, the ECO/*pABCA4* based nanoparticles are promising for non-viral gene therapy for Stargardt disease and can be expended for applications in a variety of visual dystrophies with mutated large genes.

Keywords

Non-viral gene delivery; ECO; Plasmid DNA; Gene therapy; SV40 enhancer; Stargardt disease

1. Introduction

Stargardt disease (STGD) is characterized as gradual bilateral decline in central vision and visual acuity that is commonly caused by mutations in *ABCA4* gene, which encodes a 210-kDa ATP-dependent flippase importer [1,2]. Gene replacement therapy, that delivers a healthy copy of a mutated gene into the targeted cells and expresses the encoded functional protein to restore its normal function, has shown the promise for effective treatment for STGD and other genetic ocular diseases [3–5]. The first FDA approved gene therapy is adeno-associated virus (AAV) expressing *hRPE65* for treating Leber's congenital amaurosis type 2 (LCA2) [6]. The recent success has re-energized the enthusiasm in developing gene therapy to treat previously untreatable genetic disorders. Numerous gene therapies have been developed and some are now in various phases of clinical trials [7]. Most of the gene therapies under clinical development are based on AAVs. However, the broad application of AAV-based gene therapy is limited by its cargo capacity [8,9]. This greatly restricted the application of viral gene therapies to treat ocular genetic diseases caused by mutations in large genes, such as Stargardt disease (STGD) and Usher Syndrome [10–12]. For viral systems, strategies such as dual-AAV, multi-AAV vectors, and lentiviral vectors have been tested to overcome the limitations [13–16]. Clinical application of these therapies is hindered by various limitations, including poor expression of whole functional proteins and immunogenicity. Non-viral gene delivery systems do not have limitations in gene packaging capacity and have also been developed for treating various retinal genetic diseases covering wide range of gene sizes [17,18].

A challenge for gene therapy in retinal genetic diseases is to maintain prolonged stable protein expression to retain normal visual functions. Clinically, one subretinal administration of AAV therapy could last for years in LCA2 patients, but the clinical findings indicated declining therapeutic effect over time [4,19,20]. Repetitive administrations may be needed to sustain the rescuing effect in retinal structure and function. Unfortunately, immune response development after the initial viral gene therapy renders the following repeated injection of the viral vector ineffective [21]. Non-viral gene therapy exhibits low immunogenicity and can be repeatedly administered for prolonged therapeutic efficacy. However, non-viral gene delivery systems may suffer from low efficiency [22]. The functional segments on the therapeutic gene construct can be modified to enhance the therapeutic efficacy. Because of the unlimited gene loading capacity of the non-viral system, therapeutic plasmids can be modified with tissue specific promoters to achieve specific gene expression in different retinal tissues or cells [23,24]. Tissue specific promoters have been incorporated in plasmid DNA to enhance specific gene expression, while universal promoters used in AAV-based

gene therapy tend to facilitate non-specific transient protein expression in all cell types [25,26]. Tissue specific promoters can also minimize off-target transgene expression and improve the safety of gene therapy. Therapeutic gene constructs can also be modified with expression enhancers for enhancing exogenous expression in mammalian cells with the non-viral delivery systems [27].

Development of stable and reproducible formulation of nanoparticle based non-viral gene therapy is an essential step for clinical translation based on the requirements from the regulatory agencies. The formulation or drug product of gene therapy should have consistent physicochemical properties, including acceptable stability and shelf life, consistent particle size, size distribution and surface charges [28]. It is costly to establish Good Manufacturing Practice (GMP) for viral gene therapies due to expensive biological production process, which leads to high prices for the therapies [29,30]. The GMP production of non-viral gene therapies can be achieved with conventional chemical process, which is more cost-effective than viral systems. In order to produce consistent and stable nanoparticle formulations, stabilizers have been used in the formulations to prevent particle aggregations [31,32]. Most stabilizers are able to form hydrogen bonds on the surface of nanoparticles to stabilize nanoparticle formulations in aqueous solution by either exchanging with water molecules or forming an inert and rigid glass matrix for an acceptable shelf-life [33]. The stabilizers are generally biocompatible substances with minimal effect on the nanoparticle functions. Sucrose, trehalose, sorbitol and hydroxyethyl starch have been used as stabilizers in a wide variety of nanoparticle formulations [34–36].

We have developed a multifunctional pH-sensitive amino lipid (1-aminoethyl)iminobis[N-(oleoylcysteinyl-1-amino-ethyl)propionamide) (ECO) based nanoparticle platform for efficient intracellular delivery of therapeutic nucleic acids, including siRNA and plasmid DNA. ECO has demonstrated excellent efficacy for cytosolic delivery of therapeutic nucleic acids of different sizes in a wide range of applications [25,26,33,37–44]. In a previous study, we demonstrated that ECO facilitated efficient subretinal delivery of a large rhodopsin promoter (photoreceptor specific) modified therapeutic *ABCA4* plasmid (*pRHO-ABCA4*, 12 kb), and induced long-term ABCA4 expression in the retina of a mouse model of Stargardt disease [25,26]. In this study, we optimized the therapeutic plasmid with a simian virus 40 enhancer (*SV40*) (*pRHO-ABCA4-SV40*) for prolonged gene expression. We also explored and developed stable ECO/*pRHO–ABCA4–SV40* nanoparticle formulations using sucrose and sorbitol to improve stability and shelf-life for clinical translation. The formulations of ECO/*pCMV–ABCA4–SV40* nanoparticles were also developed as a non-specific control. The nanoparticles were characterized and tested for gene expression *in vitro* and *in vivo*. Gene replacement therapy of ECO/*pRHO–ABCA4–SV40* nanoparticle formulations was also performed to evaluate the efficacy in $Abca4^{-/-}$ mice, the orthologous rodent model to STGD.

2. Results

In order to enhance the expression of *ABCA4* gene, a simian virus 40 enhancer (*SV40*) was incorporated into the *pRHO–ABCA4* vector, which was used in our previous publications [25,26]. As shown in Fig. 1A, the *SV40* enhancer was inserted in *pRHO–ABCA4*

between *NheI* and *NotI* restriction sites. The successful preparation of *pRHO–ABCA4–SV40* plasmid was confirmed by agarose gel electrophoresis showing the polyA *SV40* enhancer band after digestions at *NheI* and *NotI* restriction sites (Fig. 1B). Similarly, *pCMV–ABCA4–SV40* was also prepared as a control plasmid using the plasmid in our previous publications [25,26].

ECO/*pDNA* nanoparticles of *pRHO–ABCA4–SV40* and *pCMV–ABCA4–SV40* were first prepared by self-assembly of ECO with the plasmids at amine/phosphate (N/P) ratios of 6, 8 and 10 [25,26]. The plasmids *pRHO–ABCA4* and *pCMV–ABCA4* were used as controls. Sucrose or sorbitol were then added as an excipient with a concentration of 5% or 10% to stabilize the nanoparticles. The nanoparticles were characterized by dynamic light scattering (DLS) for their size distributions (Fig. 2) and zeta potential distributions (Fig. 3) under different excipient conditions. As shown in Fig. 2, ECO and *pABCA4s* formulated stable nanoparticles at all the N/P ratios in the presence of sucrose at both 5% and 10% contents. The sizes were between 220 nm and 250 nm and the distributions were seen as single peaks with negligible aggregation peaks and were not affected by the excipient. However, sorbitol addition affected some of the ECO/*pABCA4* formulations. For example, ECO/*pRHO–ABCA4* at N/P ratio of 6, ECO/*pRHO–ABCA4–SV40* at N/P ratio of 8, ECO/*pCMV–ABCA4* at N/P ratio of 10, and ECO/*pCMV–ABCA4–SV40* at N/P ratio of 10 showed broadened size distributions after sorbitol addition. Zeta potential distributions demonstrated no noticeable change after sucrose additions for the ECO/*pABCA4* nanoparticle formulations (Fig. 3). ECO/*pABCA4* nanoparticles demonstrated uniformed distributions around +20 mV across all the N/P ratios under sucrose conditions. However, sorbitol addition to ECO/*pABCA4* nanoparticle formulations resulted in some noticeable changes in zeta potential distributions.

Encapsulation of *pABCA4s* in the ECO/*pABCA4* nanoparticle formulations under different excipient conditions (sucrose and sorbitol, 5% or 10%) was verified by agarose gel electrophoresis (Fig. 4). ECO and *pABCA4*s formulated stable nanoparticles at all N/P ratios for all the excipients conditions, demonstrated by visible bands remaining on the top of the gels. As shown in our previous studies, ECO could efficiently encapsulate *pABCA4s* or other large plasmids with nanoparticle stability observed through the voltage conditions of electrophoresis [25,26,44]. Unlike the effects on the size and zeta potential distributions, sorbitol did not affect the stability and encapsulations of ECO/*pABCA4* nanoparticles. Taken together, sorbitol has some unpredictable effects on the stability of the ECO/*pABCA4* nanoparticles and may not be a suitable excipient for ECO/*pDNA* nanoparticles despite that it has commonly used on pharmaceutical formulations. Sucrose demonstrates no effect on the size, zeta potential and stability of ECO/*pABCA4* nanoparticles and is a promising excipient for the formulations of ECO/*pABCA4* nanoparticles.

To assess the introduction of *SV40* enhancer on transfection efficiency, ECO/*pCMV–ABCA4* and ECO/*pCMV–ABCA4–SV40* nanoparticles (N/*P* = 6, 8, 10; *pDNA* concentration 1 μg/mL and 2 μg/mL) were investigated in ARPE-19 cells. *ABCA4* expressions at the mRNA level were analyzed using qRT-PCR 48 h after transfection (Fig. 5). ECO/*pCMV–ABCA4–SV40* nanoparticles demonstrated significantly more *ABCA4 mRNA* expression than ECO/*pCMV–ABCA4* without the *SV40* enhancer for both doses.

ABCA4 mRNA expression also increased with the N/P ratios and *pDNA* doses. Therefore, introduction of the *SV40* enhancer is able to significantly enhance the *in vitro* expression of ECO/*pDNA* nanoparticle formulations.

The effect of sucrose and sorbitol on gene expression was also evaluated using *pCMV–ABCA4* (with and without *SV40* enhancer) and a reporter plasmid *pCMV–GFP* in ARPE-19 cells. The GFP expression was evaluated using confocal microscope and flow cytometry 48 h after transfection (Fig. 6). Significant GFP signals were observed under confocal for all the conditions compared with untreated control using ECO/*pCMV–GFP* nanoparticles (Fig. 6A). The flow cytometry results also demonstrated around 70% of cells showing GFP expression for ECO/*pCMV–GFP* nanoparticles in 5%, 10% sucrose and 10% sorbitol (Fig. 6B and C). However, GFP expression was significantly reduced when 5% sorbitol was added (Fig. 6C). *ABCA4* expression were not affected by sucrose addition as demonstrated in Fig. 6D. ECO/*pCMV–ABCA4–SV40* nanoparticles demonstrated significantly higher *ABCA4* mRNA expression than ECO/*pCMV–ABCA4* due to the effect of the introduction of *SV40* enhancer. However, sorbitol addition significantly reduced the *ABCA4* mRNA expression for ECO/*pCMV–ABCA4–SV40* nanoparticles (Fig. 6D). The results indicated that *SV40* enhancer could enhance *ABCA4* expression *in vitro* and sucrose had no effect on the transfection efficiency of ECO/*pDNA* nanoparticles, while sorbitol demonstrated unpredictable effects on ECO/*pDNA* transfection efficiency.

The cytotoxicity of ECO/*pDNA* nanoparticles were evaluated using *pRHO–ABCA4* and *pCMV–ABCA4* (with or without enhancer *SV40*) at different N/P ratios (6 and 8) and different doses in ARPE-19 cells. As shown in Fig. 7, ECO/*pRHO–ABCA4* (with and without enhancer) demonstrated better cell viability than ECO/*pCMV–ABCA4* (with and without enhancer). Higher *pDNA* doses were correlated with lower cell viabilities across all the nanoparticles. At N/P ratio of 6, almost all nanoparticles demonstrated more than 80% cell viability, except for higher doses groups. At N/P ratio of 8, reduced cell viability was observed for higher doses, especially for *pCMV–ABCA4*. Overall, ECO/*pABCA4* nanoparticles demonstrated good cell viability and low cytotoxicity.

The efficacy of preventing Stargardt disease (STGD) progression using gene therapy with ECO/*pRHO–ABCA4* and ECO/*pRHO–ABCA4–SV40* was assessed based on the accumulation of A2E in the retinal pigmented epithelium (RPE) of *Abca4*$^{-/-}$ mice. A2E, a photo-toxic dimer of vitamin A, is a main component of lipofuscin. A2E accumulation is commonly used as an indicator of STGD progression [45,46]. One of the therapeutic strategies for treating STGD is to slow down the production of A2E to minimize chronic oxidative damage that ultimately leads to atrophy. In previous work, we demonstrated prolonged ABCA4 expression in *Abca4*$^{-/-}$ mice and reduced A2E accumulation [25]. Similarly, the *Abca4*$^{-/-}$ mice (1-month-old) received a single subretinal injection of ECO/*pRHO–ABCA4* or ECO/*pRHO–ABCA4–SV40* with PBS as a control. All the treated mice were euthanized 8 months after injection and the A2E levels were analyzed using high-performance liquid chromatography (HPLC). A2E was identified as the peak at 2.5 min in the chromatograms under current HPLC running conditions, which was ensured by the analysis of the synthesized A2E standard (Fig. 8A). The spectra of A2E standard, A2E from control, ECO/*pRHO–ABCA4* treated, and ECO/*pRHO–ABCA4–SV40* treated

mice were compared and found to contain the same peaks at 336 nm and 439 nm (Fig. 8B). The area of A2E peaks reduced significantly after treatments of ECO/*pRHO–ABCA4* and ECO/*pRHO–ABCA4–SV40* nanoparticles compared with the control group (Fig. 8C). Quantitative analysis demonstrated an average A2E level of 71.78 ± 25.60% (*ca.* 29% reduction) for ECO/*pRHO–ABCA4–SV40* and 63.95 ± 27.54% (*ca.* 36% reduction) for ECO/*pRHO–ABCA4* treated mice (Fig. 8D). A large variation of *in vivo* efficacy was observed with ECO/*pRHO–ABCA4–SV40* nanoparticles. The modification of *pRHO–ABCA4* with the *SV40* enhancer did not result in improvement of *in vivo* efficacy than the unmodified plasmid. This could be explained from the *ABCA4* mRNA expression after subretinal treatments using ECO/*pRHO–ABCA4* and ECO/*pRHO–ABCA4–SV40* nanoparticles. ECO/*pRHO–ABCA4–SV40 resulted in slightly higher ABCA4* mRNA expression than ECO/*pRHO–ABCA4* at 4 days although difference was not significant (Fig. 8E). In contrast, *ABCA4* mRNA expression with ECO/*pRHO–ABCA4–SV40 was slightly less* than ECO/*pRHO–ABCA4* at 4.5 months (Fig. 8F). It implies that the plasmid *pRHO–ABCA4–SV40* with the viral enhancer might be cleared faster than the one without the enhancer.

3. Discussion

Gene therapy holds great promise for the treatment of monogenic retinal disorders, but still faces challenges for efficient and specific delivery of therapeutic genes, especially large genes. The clinical applications of adeno-associated viruses (AAVs) are limited to the genes that can fit in the viral cavities. The multifunctional pH-sensitive amino lipid ECO can encapsulate genetic materials of unlimited sizes from siRNAs and miRNAs to large plasmid DNAs [25,26,37–44]. ECO has demonstrated high transfection efficiency both *in vitro* and *in vivo* for various applications from cancer therapies to retinal gene therapies [25,26,37–44]. ECO based nanoparticles can facilitate pH-sensitive amphiphilic endosomal membrane destabilization and endosomal escape as well as reductive dissociation of the nanoparticles to release nucleic acids in cytoplasm, the PERC effect, which allows highly efficient cytosolic delivery of therapeutic nucleic acids [25,26,37–44]. Here, ECO readily formed stable nanoparticles with *ABCA4* plasmids *via* self-assembly with uniformed size distributions and complete encapsulations, and mediated efficient intracellular gene delivery and expression.

Clinical translation of nanoparticle-based non-viral gene therapies for retinal genetic disorders requires the development of stable nanoparticle formulations to ensure safety and efficacy of drug products. Excipients are commonly used in nanoparticle formulations to preserve the nanoparticles with consistent physicochemical properties. Sucrose and sorbitol are the commonly used excipients for the stabilization of the nucleic acid nanoparticle formulations. Interestingly, we found in this work that they behaved differently on the stability of the ECO/*pDNA* nanoparticles. Although the presence of both excipients resulted in complete encapsulation of the DNA plasmids in the nanoparticles, sorbitol caused substantial aggregation and change of zeta potentials of the nanoparticles in aqueous solution, while sucrose did not have a noticeable effect on particle formulations (Figs. 2, 3 and 4). Sucrose has been tested previously as a stabilizer for ECO/siRNA nanoparticles, which also demonstrated no negative effects on particle formulations, retained transfection

efficiency, and improvements in nanoparticle long-term storage [33]. The formulations with sucrose also resulted in higher expression of a reporter gene and *ABCA4* than those with sorbitol. The difference between sucrose and sorbitol may be associated with their structures. Sucrose is a disaccharide of glucose and fructose, which can form an inert and rigid glass matrix that can immobilize the nanoparticles to stabilize the formulation [47]. Sorbitol is linear polyols but possibly facilitates the nanoparticles *via* hydrogen binding [48].

The *pRHO–ABCA4* plasmid was modified by adding an enhancer *SV40* with an expectation of augmenting the gene expression for efficacious treatment of Stargardt disease. We have shown previously that ECO/*pRHO–ABCA4* was effective to mediate gene expression specifically in the outer segments of the photoreceptor cells. The tissue specific bovine rhodopsin specific promoter (*RHO*) in the plasmid facilitates specific expression of ABCA4 in the outer segment (OS) previously [25]. Enhancer sequences are often incorporated in the plasmid DNA to increase gene expression with non-viral nanoparticles. The *SV40* enhancer containing a 72 base pair repeat could enhance the expression of nonviral genes in cells and *in vivo* [49,50]. It was incorporated in *pRHO-ABCA4–SV40* to explore the potential for enhanced long-term expression of ABCA4 for treating Stargardt disease. Since it is difficult to culture photoreceptor cells, we constructed a different plasmid with a common *CMV* promotor and *SV40* enhancer (*pCMV–ABCA4–SV40*) to assess the effect of *SV40* enhancer *in vitro* with ARPE-19 cells. Significantly augmented gene expression was observed for ECO/*pCMV–ABCA4–SV40* when compared to ECO/*pCMV–ABCA4* (Fig. 5).

We have shown previously that ECO/*pRHO–ABCA4* nanoparticles can induce up to 8-month expression of ABCA4 in mice and can delay the disease progression by reducing A2E accumulation in *Abca4*$^{-/-}$ mice [25]. The efficacy of ECO/*pRHO–ABCA4–SV40* was assessed in comparison with ECO/*pRHO–ABCA4* at 8 months after a single subretinal injection in *Abca4*$^{-/-}$ mice. Both nanoparticles demonstrated about 29% and 36% A2E reduction on average compared to the PBS injected controls (Fig. 8). No significant difference was observed between ECO/*pRHO–ABCA4–SV40* and ECO/*pRHO–ABCA4* as was shown in the *in vitro* experiments. The inclusion of the *SV40* enhancer did not demonstrate better efficacy, possibly due to the cell type preference of *SV40* and the fluctuating nature of the virus origin [51]. Another explanation could be fast clearance of the *pRHO–ABCA4–SV40* plasmid with the viral enhancer from the eye based on the reduction of mRNA expression in the eye over time, (Fig. 8E,F). The other cause could be the variability for subretinal injections, which is a challenging task as well. Nevertheless, the observation is helpful to explore different strategies on the optimization of the *ABCA4* plasmid for enhanced therapeutic efficacy. Currently, we are exploring modifications of *ABCA4* plasmid with a human promoter and a human enhancer for clinical translation.

In conclusion, multifunctional pH-sensitive amino lipid ECO and *ABCA4* plasmids form stable nanoparticle formulations through self-assembly in both 5% and 10% sucrose stabilizer. The addition of sucrose as stabilizer produced no effect on the transfection efficiency of ECO/*pABCA4* nanoparticles. Modification of *ABCA4* plasmids with an *SV40* enhancer induced significantly higher gene expression in ARPE-19 cells, and demonstrated a similar level of A2E reduction in treated *Abca4*$^{-/-}$ mice as ECO/*pRHO–ABCA4* nanoparticles. Therefore, the ECO/*pABCA4* nanoparticles with a modified enhancer

sequence and the stabilizer can be a promising, reliable, and safe non-viral gene therapy platform to deliver large therapeutic genes for the treatment of Stargardt disease.

4. Materials and methods

4.1. Reagents

All reagents ordered from vendors were directly used without extra purification unless they were otherwise detailed in this section. Organic solvents such as, acetonitrile (ACN), ethanol and methanol were ordered from Thermo Fisher Scientific (Hampton, NH). The synthesis of Lipid ECO followed the procedures reported previously [37,38]. For cell culture, penicillin fetal bovine serum, and streptomycin were purchased from Invitrogen (Carlsbad, CA). The *ABCA4* plasmid (*pCMV–ABCA4*) was kindly gifted by Dr. Robert S. Molday (University of British Columbia), which included human *ABCA4* cDNA sequence of full-length (NCBI Accession # NM_000350.2) on a *pCEP4* backbone. *pRHO–ABCA4* was prepared as previously described [25].

4.2. Plasmid construction

The *pRHO–ABCA4* plasmid was constructed by molecular cloning of the cDNA for the *ABCA4* gene into the linearized *pRHO–DsRed* plasmid with the *DsRed* reporter gene removed [25]. The cDNA for the *ABCA*4 gene was amplified by polymerase chain reaction (PCR) with the Q5 High-Fidelity DNA Polymerase enzyme. The forward primer was 5'-AATACCGGTATGGGCTTCGTGAGACAGATA-3′ and the reverse primer was 5′-TATATAGCGGCCGCTAGCTCAGTCTGCTGTTT-3′ for adding the *AgeI* and *NotI* restriction sites to the 5′- and 3′-ends of *ABCA4*, respectively. All enzymes were purchased from New England Biolabs (Ipswich, MA). *SV40* polyA and *SV40* enhancer was copied from plasmid *pGL3*-control vector (Promega, Madison, WI) by PCR with forward primer 5′-ATGCGGCCGCTACCACATTTGTAGAGGTTTTAC and reverse primer 5′-AAGCTAGCGCTGTGGAATGTGTGTCAG containing *NotI* and *NheI* sites on both ends. Digested and purified *SV40* polyA and enhancer fragment was ligated to *pRHO–ABCA4* plasmid. Final plasmid stocks were confirmed by Sanger sequencing.

4.2.1. Cell culture—ARPE-19 (ATCC, Manassas, Virginia) cells were passaged and maintained in a Dulbecco's modified Eagle's medium containing fetal bovine serum (10%), streptomycin (100 μg/mL), and penicillin (100 units/mL). Cells were kept in a humidified incubator at 37 °C and 5% CO_2.

4.2.2. Animal—Pigmented *Abca4*$^{-/-}$ knockout mice were obtained as described previously and maintained with mixed backgrounds of 129Sv/Ev or C57BL/6 [25,26]. Animals were housed and bred in the Animal Resource Center at CWRU. All procedures followed approved protocols by the CWRU Institutional Animal Care and Use Committee (IACUC#2014–0053), which were also in compliance with recommendations from the Association for Research for Vision and Ophthalmology and the American Veterinary Medical Association Panel on Euthanasia.

4.2.3. Preparation of ECO/pDNA nanoparticles—The preparation of ECO/*pDNA* nanoparticles was as previously described [25,26]. Briefly, ECO (25 mM) in ethanol was added and mixed with a plasmid DNA (0.5 mg/mL) aqueous solution at predetermined volume from the N/P ratio (amine to phosphate ratio) of 6, 8 or 10. The mixture was first vortexed at 3000 rpm for 1 min and left on a shaker for 30 min. For some of the nanoparticles, sucrose (5% or 10%) or sorbitol (5% or 10%) was added after the first shaking and further shaken for another 20 min. The final DNA concentration in the nanoparticle for characterization and *in vivo* experiments was 200 ng/μL. For *in vitro* transfection, an ECO stock solution of 2.5 mM was used to formulate nanoparticles. Encapsulations of *pDNA* by lipid ECO in nanoparticle formulations were characterized by an agarose gel electrophoresis method. Agarose gel (0.7%) in TBE buffer (0.5%) was performed at 120 V for 25 min.

4.2.4. Dynamic light scattering—The sizes and zeta potentials were characterized for nanoparticle formulations of ECO/*pDNA* using a dynamic light scattering method with an Anton Paar Litesizer 500 (Anton Paar USA Inc., Ashland, VA). Each sample was analyzed at 25 °C.

4.2.5. In vitro transfection—Transfections were performed on 12-well plates, where ARPE-19 cells were seeded at a concentration of 4×10^4 cells/well. Cells were allowed to grow for 24 h before transfection. Nanoparticles of different N/P ratios at *pDNA* concentrations of 1 or 2 μg/mL in DMEM with 10% serum were added to ARPE-19 cells and incubated for 8 h at 37 °C. The media containing nanoparticles was then replaced with fresh DMEM (10% serum). ARPE-19 cells were further incubated for an additional 48 h. Expression of *ABCA4* was evaluated by qRT-PCR at mRNA level.

Transfection of ECO/*pCMV–GFP* nanoparticles of N/*P* = 8 was also conducted similarly in ARPE-19 cells, where DMEM (10% serum) and a *pDNA* concentration of 1 μg/mL were used. The transfection was performed in a 12-well plate with ARPE-19 cell concentration of 4×10^4 cells per well. The nanoparticles were incubated with ARPE-19 cells as previously described. After 48 h, fluorescence images of GFP expression were acquired using an Olympus FV1000 confocal microscope.

4.2.6. Cytotoxicity—Cytotoxicity of ECO/*pABCA4* nanoparticles was investigated using a CCK-8 assay (Dojindo Molecular Technologies, Inc., Washington, D.C.). Cell viability was evaluated using ARPE-19 cells on 96-well plates, where cells were seeded at a concentration of 1×10^4 cells per well. ARPE-19 cells were incubated with ECO/*pABCA4* nanoparticles at different DNA doses of (10 ng, 25 ng, 50 ng, 100 ng, 200 ng, 400 ng, and 800 ng) in 100 μL DMEM (10% serum) medium for 8 h at 37 °C. Then the nanoparticle containing DMEM was replaced with fresh DMEM (10% serum). The cells were allowed to grow until 48 h and washed with PBS. The CCK-8 reagent was added to each well followed by an incubated of 1.5 h at 37 °C. The absorbance at 450 nm was recorded using a plate reader. Cell viability was characterized by normalizing to the absorption of non-treated control.

4.2.7. qRT-PCR—The analysis was performed as previously described [25,26]. A scraper was used for cell lysis and homogenization. The RNA extractions for cell samples were conducted using a QIAGEN RNeasy kit following the manufacturer's instructions. cDNAs were synthesized from mRNA transcripts using a QIAGEN miScriptII reverse transcriptase kit (Germantown, MD). For animal experiments, the eye tissue samples were homogenized using a glass tube loaded with 0.6 mL of the lysis buffer on ice. The RNA extractions and cDNAs synthesis were performed using the same kits as described previously for cell samples. The qRT-PCR analysis was performed in a Mastercycler instrument (Eppendorf, Hauppauge, NY) using a SYBR Green Master mix (AB Biosciences, Allston, MA). Fold changes of mRNA levels were determined by normalization to 18S. Primers for *ABCA4* can be found in previous work [25].

4.2.8. In vivo subretinal transfection with ECO/pDNA nanoparticles—Subretinal injection was performed as previously described [25]. The nanoparticle solution (1 μL) was injected by a pump with a steady speed of 150 nL/s into the mouse eye. Successful administration was confirmed by bleb formation in the subretinal space. A total of 200 ng plasmid or *pABCA4* was delivered. Mice injected with 1 μL of PBS were used as controls.

4.3. Synthesis and HPLC analysis of A2E

Synthesis of A2E standard was the same as described previously [25]. A mixture of all-*trans*-retinal (100 mg, 352 μmol) and ethanolamine (9.5 mg, 155 μmol) in ethanol (3.0 mL) was stirred in the presence of acetic acid (9.3 μL, 155 μmol) at room temperature with a sealed cap in the dark for 2 days. After the mixture was concentrated *in vacuo*, the residue was purified by silica gel column chromatography. After elution with MeOH:CH_2Cl_2 (5:95), further elution with MeOH: CH_2Cl_2: trifluoroacetic acid (8:92:0.001) gave A2E. Pure samples were obtained by HPLC purification [ZORBAX 300 SB-C18, 9.4 × 250 mm, 84–100% water/acetonitrile for 30 min, 1.0 mL/min flow detected at UV 430 nm]. A2E was detected at retention time (t_R = 35.2 min). Collection of the fraction provided pure A2E for further analysis. A2E was characterized by mass spectrometry.

A2E samples were extracted from the deep-frozen (−80 °C) eye samples. The extraction was performed in 1 mL of acetonitrile after homogenization with a Brinkmann Politron homogenizer (Kinematica, Lucerne, Switzerland). After evaporation of solvent, extracts were dissolved in 120 μL acetonitrile with 0.1% TFA. Samples (100 μL) were loaded on a C18 column (Gemini® 5 μm 110 Å HPLC Column 250 × 4.6 mm) (Phenomenex, Torrance, CA) and analyzed by an Agilent 1260 infinity II reverse-phase HPLC (Agilent Technologies, Santa Clara, CA). A2E was eluted with the following gradients of acetonitrile in water (containing 0.1% trifluoroacetic acid): 85–96% (10 min), 96% (5 min), 96–100% (2 min), and 100% (13 min) (flow rate, 1 mL/min), and they were monitored at 439 nm. For A2E quantification by reverse phase HPLC, areas of the A2E peaks from the treated mice were normalized to the average of controls. Total of 4 ECO/*pRHO–ABCA4* treated eyes, 5 ECO/*pRHO–ABCA4–SV40* treated eyes and 10 control eyes were analyzed.

4.3.1. Statistical analysis—Experiments were performed in triplicate and the number of animals is listed in the figure captions. Experimental data are presented as averages with standard deviations. Statistical analysis was performed with one-way ANOVA and two-tailed Student's *t*-tests. A 95% confidence interval was used and $P \leq 0.05$ was accepted as statistically significant.

Acknowledgements

This project was supported by the Gund-Harrington Scholars Award from the Harrington Discovery Institute and by the Foundation Fighting Blindness. Further support was obtained through grants from the NIH (NEI R24-EY-024864 and NEI R24-EY-027283), the Canadian Institute for Advanced Research (CIFAR), the Alcon Research Institute (ARI), unrestricted grants from Research to Prevent Blindness to the Departments of Ophthalmology at UCI, Grant BX003604 from the Department of Veterans Affairs. K.P. is Chief Scientific Officer of Polgenix Inc. Z.R.L. is an M. Frank Rudy and Margaret Domiter Rudy Professor of Biomedical Engineering.

References

[1]. Sullivan JM, Focus on molecules: ABCA4 (ABCR)–an import-directed photoreceptor retinoid flipase, Exp. Eye Res. 89 (5) (2009) 602–603. [PubMed: 19306869]

[2]. Wiszniewski W, Zaremba CM, Yatsenko AN, Jamrich M, Wensel TG, Lewis RA, Lupski JR, ABCA4 mutations causing mislocalization are found frequently in patients with severe retinal dystrophies, Hum. Mol. Genet. 14 (19) (2005) 2769–2778. [PubMed: 16103129]

[3]. Schimmer J, Breazzano S, Investor outlook: significance of the positive LCA2 gene therapy phase III results, Human Gene Therapy Clin. Dev 26 (4) (2015) 208–210.

[4]. Simonelli F, Maguire AM, Testa F, Pierce EA, Mingozzi F, Bennicelli JL, Rossi S, Marshall K, Banfi S, Surace EM, Sun J, Redmond TM, Zhu X, Shindler KS, Ying G-S, Ziviello C, Acerra C, Wright JF, McDonnell JW, High KA, Bennett J, Auricchio A, Gene therapy for Leber's congenital amaurosis is safe and effective through 1.5 years after vector administration, Mol. Ther. 18 (3) (2010) 643–650. [PubMed: 19953081]

[5]. Koirala A, Conley SM, Makkia R, Liu Z, Cooper MJ, Sparrow JR, Naash MI, Persistence of non-viral vector mediated RPE65 expression: case for viability as a gene transfer therapy for RPE-based diseases, J. Control. Release 172 (3) (2013) 745–752. [PubMed: 24035979]

[6]. Prado DA, Acosta-Acero M, Maldonado RS, Gene therapy beyond luxturna: a new horizon of the treatment for inherited retinal disease, Curr. Opin. Ophthalmol. 31 (3) (2020).

[7]. Lipinski DM, Thake M, MacLaren RE, Clinical applications of retinal gene therapy, Prog. Retin. Eye Res 32 (2013) 22–47. [PubMed: 22995954]

[8]. Wu Z, Yang H, Colosi P, Effect of genome size on AAV vector packaging, Mol. Therapy 18 (1) (2010) 80–86.

[9]. Santiago-Ortiz JL, Schaffer DV, Adeno-associated virus (AAV) vectors in cancer gene therapy, J. Control. Release 240 (2016) 287–301. [PubMed: 26796040]

[10]. Schulz HL, Grassmann F, Kellner U, Spital G, Rüther K, Jägle H, Hufendiek K, Rating P, Huchzermeyer C, Baier MJ, Weber BHF, Stöhr H, Mutation Spectrum of the ABCA4 gene in 335 Stargardt disease patients from a multicenter German cohort-impact of selected deep Intronic variants and common SNPs, Invest. Ophthalmol. Vis. Sci. 58 (1) (2017) 394–403. [PubMed: 28118664]

[11]. Williams DS, Usher syndrome: animal models, retinal function of usher proteins, and prospects for gene therapy, Vis. Res 48 (3) (2008) 433–441. [PubMed: 17936325]

[12]. Delplace V, Payne S, Shoichet M, Delivery strategies for treatment of age-related ocular diseases: from a biological understanding to biomaterial solutions, J. Control. Release 219 (2015) 652–668. [PubMed: 26435454]

[13]. Palfi A, Chadderton N, McKee AG, Blanco Fernandez A, Humphries P, Kenna PF, Farrar GJ, Efficacy of Codelivery of dual AAV2/5 vectors in the murine retina and Hippocampus, Hum. Gene Ther. 23 (8) (2012) 847–858. [PubMed: 22545762]

[14]. Maddalena A, Colella P, Trapani I, Minopoli R, Iodice C, Auricchio A, Triple AAV vectors to expand AAV cargo capacity in the retina, Invest. Ophthalmol. Vis. Sci. 56 (7) (2015) 3631.

[15]. Allocca M, Garcia-Hoyos M, Doria M, Petrillo M, Kim S, Maguire A, Vicino UD, Sparrow JR, Bennett J, Auricchio A, Gene therapy of a mouse model of Stargardt's disease using Adeno-associated viral vectors packaging large genes, Invest. Ophthalmol. Vis. Sci. 49 (13) (2008) 1129.

[16]. Miyoshi H, Takahashi M, Gage FH, Verma IM, Stable and efficient gene transfer into the retina using an HIV-based lentiviralvector, Proc. Natl. Acad. Sci. 94 (19) (1997) 10319–10323. [PubMed: 9294208]

[17]. Bordet T, Behar-Cohen F, Ocular gene therapies in clinical practice: viral vectors and nonviral alternatives, Drug Discov. Today 24 (8) (2019) 1685–1693. [PubMed: 31173914]

[18]. Mashal M, Attia N, Martinez-Navarrete G, Soto-Sanchez C, Fernandez E, Grijalvo S, Eritja R, Puras G, Pedraz JL, Gene delivery to the rat retina by nonviral vectors based on chloroquine-containing cationic niosomes, J. Control. Release 304 (2019) 181–190. [PubMed: 31071372]

[19]. Bennett J, Ashtari M, Wellman J, Marshall KA, Cyckowski LL, Chung DC, McCague S, Pierce EA, Chen Y, Bennicelli JL, Zhu X, Ying G.-s., Sun J, Wright JF, Auricchio A, Simonelli F, Shindler KS, Mingozzi F, High KA, Maguire AM, AAV2 gene therapy readministration in three adults with congenital blindness, Sci. Transl. Med 4 (120) (2012), 120ra15–120ra15.

[20]. Pierce EA, Bennett J, The status of RPE65 gene therapy trials: safety and efficacy, Cold Spring Harbor Persp. Med 5 (9) (2015).

[21]. Federico M, Katherine AH, Immune responses to AAV in clinical trials, Curr. Gene Therapy 11 (4) (2011) 321–330.

[22]. Zulliger R, Conley SM, Naash MI, Non-viral therapeutic approaches to ocular diseases: an overview and future directions, J. Control. Release 219 (2015) 471–487. [PubMed: 26439665]

[23]. Ye G-J, Budzynski E, Sonnentag P, Nork TM, Sheibani N, Gurel Z, Boye SL, Peterson JJ, Boye SE, Hauswirth WW, Chulay JD, Cone-specific promoters for gene therapy of Achromatopsia and other retinal diseases, Hum. Gene Ther. 27 (1) (2015) 72–82.

[24]. Beltran WA, Cideciyan AV, Boye SE, Ye G-J, Iwabe S, Dufour VL, Marinho LF, Swider M, Kosyk MS, Sha J, Boye SL, Peterson JJ, Witherspoon CD, Alexander JJ, Ying G-S, Shearman MS, Chulay JD, Hauswirth WW, Gamlin PD, Jacobson SG, Aguirre GD, Optimization of retinal gene therapy for X-linked retinitis Pigmentosa due to RPGR mutations, Mol. Ther. 25 (8) (2017) 1866–1880. [PubMed: 28566226]

[25]. Sun D, Schur RM, Sears AE, Gao S-Q, Vaidya A, Sun W, Maeda A, Kern T, Palczewski K, Lu Z-R, Non-viral gene therapy for Stargardt disease with ECO/pRHO-ABCA4 self-assembled nanoparticles, Mol. Ther. 28 (1) (2020) 293–303. [PubMed: 31611143]

[26]. Sun D, Schur RM, Sears AE, Gao S-Q, Sun W, Naderi A, Kern T, Palczewski K, Lu Z-R, Stable retinoid analogue targeted dual pH-sensitive smart lipid ECO/pDNA nanoparticles for specific gene delivery in the retinal pigment epithelium, ACS Appl. Bio. Mater. 3 (5) (2020) 3078–3086.

[27]. Ostad-Saffari E, Moosajee M, Wong SP, Tracey-White DC, Tolmachova T, Harbottle RP, Seabra MC, Persistent expression of non-viral S/MAR vectors in the RPE for Choroideremia gene therapy, Invest. Ophthalmol. Vis. Sci. 51 (13) (2010) 3122.

[28]. Ragelle H, Danhier F, Préat V, Langer R, Anderson DG, Nanoparticle-based drug delivery systems: a commercial and regulatory outlook as the field matures, Exp. Opin. Drug Deliv 14 (7) (2017) 851–864.

[29]. Rodrigues GA, Shalaev E, Karami TK, Cunningham J, Slater NKH, Rivers HM, Pharmaceutical development of AAV-based gene therapy products for the eye, Pharm. Res. 36 (2) (2018) 29. [PubMed: 30591984]

[30]. Clément N, Grieger JC, Manufacturing of recombinant adeno-associated viral vectors for clinical trials, Mol. Therapy Methods Clin. Dev. 3 (2016) 16002.

[31]. Abdelwahed W, Degobert G, Stainmesse S, Fessi H, Freeze-drying of nanoparticles: formulation, process and storage considerations, Adv. Drug Deliv. Rev. 58 (15) (2006) 1688–1713. [PubMed: 17118485]

[32]. Fonte P, Reis S, Sarmento B, Facts and evidences on the lyophilization of polymeric nanoparticles for drug delivery, J. Control. Release 225 (2016) 75–86. [PubMed: 26805517]

[33]. Ayat NR, Sun Z, Sun D, Yin M, Hall RC, Vaidya AM, Liu X, Schilb AL, Scheidt JH, Lu Z-R, Formulation of biocompatible targeted ECO/siRNA nanoparticles with long-term stability for clinical translation of RNAi, Nucleic Acid Therap 29 (4) (2019) 195–207. [PubMed: 31140918]

[34]. Bonaccorso A, Musumeci T, Carbone C, Vicari L, Lauro MR, Puglisi G, Revisiting the role of sucrose in PLGA-PEG nanocarrier for potential intranasal delivery, Pharm. Dev. Technol 23 (3) (2018) 265–274. [PubMed: 28128676]

[35]. Doktorovova S, Shegokar R, Souto EB, Chapter 30 - Role of Excipients in formulation development and biocompatibility of lipid nanoparticles (SLNs/NLCs), in: Ficai D, Grumezescu AM (Eds.), Nanostructures for Novel Therapy, Elsevier, 2017, pp. 811–843.

[36]. Molavi F, Barzegar-Jalali M, Hamishehkar H, Polyester based polymeric nano and microparticles for pharmaceutical purposes: a review on formulation approaches, J. Control. Release 320 (2020) 265–282. [PubMed: 31962095]

[37]. Malamas AS, Gujrati M, Kummitha CM, Xu R, Lu Z-R, Design and evaluation of new pH-sensitive amphiphilic cationic lipids for siRNA delivery, J. Control. Release 171 (3) (2013) 296–307. [PubMed: 23796431]

[38]. Gujrati M, Malamas A, Shin T, Jin E, Sun Y, Lu Z-R, Multifunctional cationic lipid-based nanoparticles facilitate Endosomal escape and reduction-triggered cytosolic siRNA release, Mol. Pharm. 11 (8) (2014) 2734–2744. [PubMed: 25020033]

[39]. Sun D, Sahu B, Gao S, Schur RM, Vaidya AM, Maeda A, Palczewski K, Lu ZR, et al., Mol. Therapy Nucleic Acids 7 (2017) 42–52. [PubMed: 28624218]

[40]. Sun D, Maeno H, Gujrati M, Schur R, Maeda A, Maeda T, Palczewski K, Lu ZR, Self-assembly of a multifunctional lipid with Core–Shell Dendrimer DNA nanoparticles enhanced efficient gene delivery at low charge ratios into RPE cells, Macromol. Biosci 15 (12) (2015) 1663–1672. [PubMed: 26271011]

[41]. Gujrati M, Vaidya A, Lu Z-R, Multifunctional pH-sensitive amino lipids for siRNA delivery, Bioconjug. Chem 27 (1) (2016) 19–35. [PubMed: 26629982]

[42]. Sun D, Schur RM, Lu Z-R, A novel nonviral gene delivery system for treating Leber's congenital amaurosis, Ther. Deliv 8 (10) (2017) 823–826. [PubMed: 28944740]

[43]. Vaidya AM, Sun Z, Ayat N, Schilb A, Liu X, Jiang H, Sun D, Scheidt J, Qian V, He S, Gilmore H, Schiemann WP, Lu Z-R, Systemic delivery of tumor-targeting siRNA nanoparticles against an oncogenic LncRNA facilitates effective triplenegative breast Cancer therapy, Bioconjug. Chem 30 (3) (2019) 907–919. [PubMed: 30739442]

[44]. Sun D, Sun Z, Jiang H, Vaidya AM, Xin R, Ayat NR, Schilb AL, Qiao PL, Han Z, Naderi A, Lu Z-R, Synthesis and evaluation of pH-sensitive multifunctional lipids for efficient delivery of CRISPR/Cas9 in gene editing, Bioconjug. Chem 30 (3) (2019) 667–678. [PubMed: 30582790]

[45]. Brunk UT, Terman A, Lipofuscin: mechanisms of age-related accumulation and influence on cell function12 1Guest Editor: Rajindar S. Sohal 2 This article is part of a series of reviews on "Oxidative Stress and Aging." The full list of papers may be found on the homepage of the journal, Free Radic. Biol. Med. 33 (5) (2002) 611–619. [PubMed: 12208347]

[46]. Radu RA, Mata NL, Nusinowitz S, Liu X, Sieving PA, Travis GH, Treatment with isotretinoin inhibits lipofuscin accumulation in a mouse model of recessive Stargardt's macular degeneration, Proc. Natl. Acad. Sci. 100 (8) (2003) 4742–4747. [PubMed: 12671074]

[47]. Anhorn MG, Mahler H-C, Langer K, Freeze drying of human serum albumin (HSA) nanoparticles with different excipients, Int. J. Pharm. 363 (1) (2008) 162–169. [PubMed: 18672043]

[48]. Piedmonte DM, Summers C, McAuley A, Karamujic L, Ratnaswamy G, Sorbitol crystallization can Lead to protein aggregation in frozen protein formulations, Pharm. Res. 24 (1) (2007) 136–146. [PubMed: 17109212]

[49]. Moreau P, Hen R, Wasylyk B, Everett R, Gaub MP, Chambon P, The SV40 72 base repair repeat has a striking effect on gene expression both in SV40 and other chimeric recombinants, Nucleic Acids Res. 9 (22) (1981) 6047–6068. [PubMed: 6273820]

[50]. Xu Z-L, Mizuguchi H, Ishii-Watabe A, Uchida E, Mayumi T, Hayakawa T, Strength evaluation of transcriptional regulatory elements for transgene expression by adenovirus vector, J. Control. Release 81 (1) (2002) 155–163. [PubMed: 11992688]

[51]. de Villiers J, Olson L, Tyndall C, Schaffner W, Transcriptional ‘enhancers’ from SV40 and polyoma virus show a cell type preference, Nucleic Acids Res. 10 (24) (1982) 7965–7976. [PubMed: 6298703]

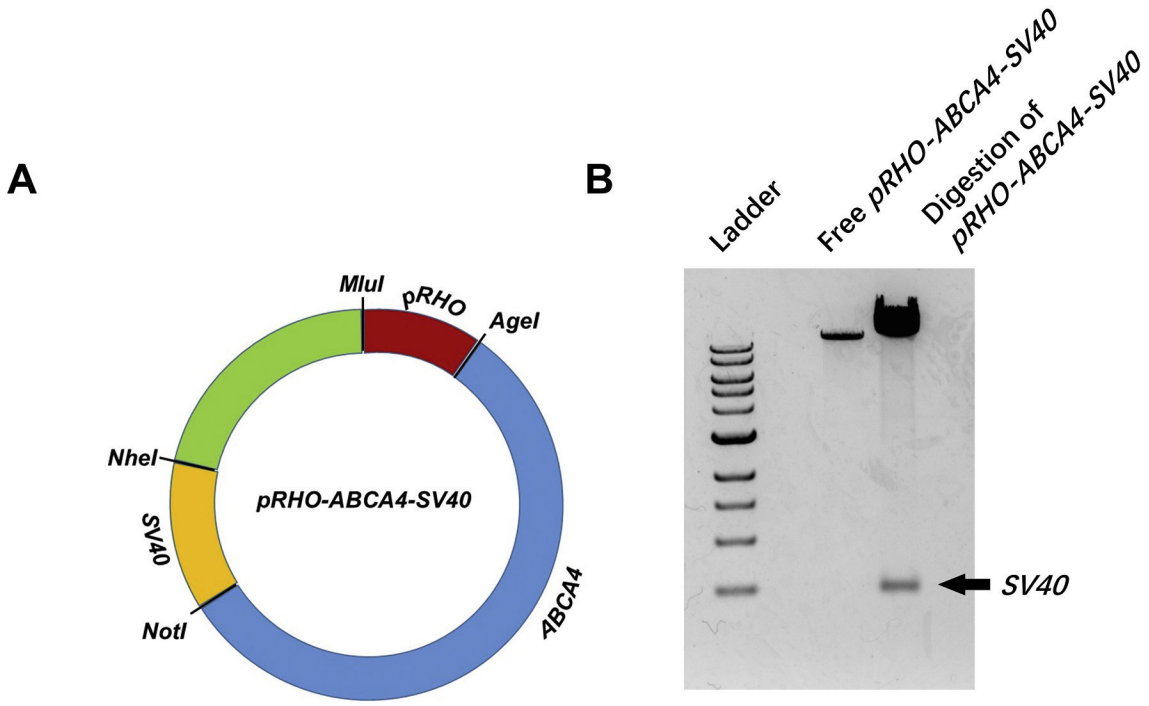

Fig. 1.

Plasmid *pRHO–ABCA4–SV40* vector map demonstrating the insertion of *SV40* enhancer between *NheI* and *NotI* restriction cites (A) and agarose gel electrophoresis confirming the success of SV40 insertion (B).

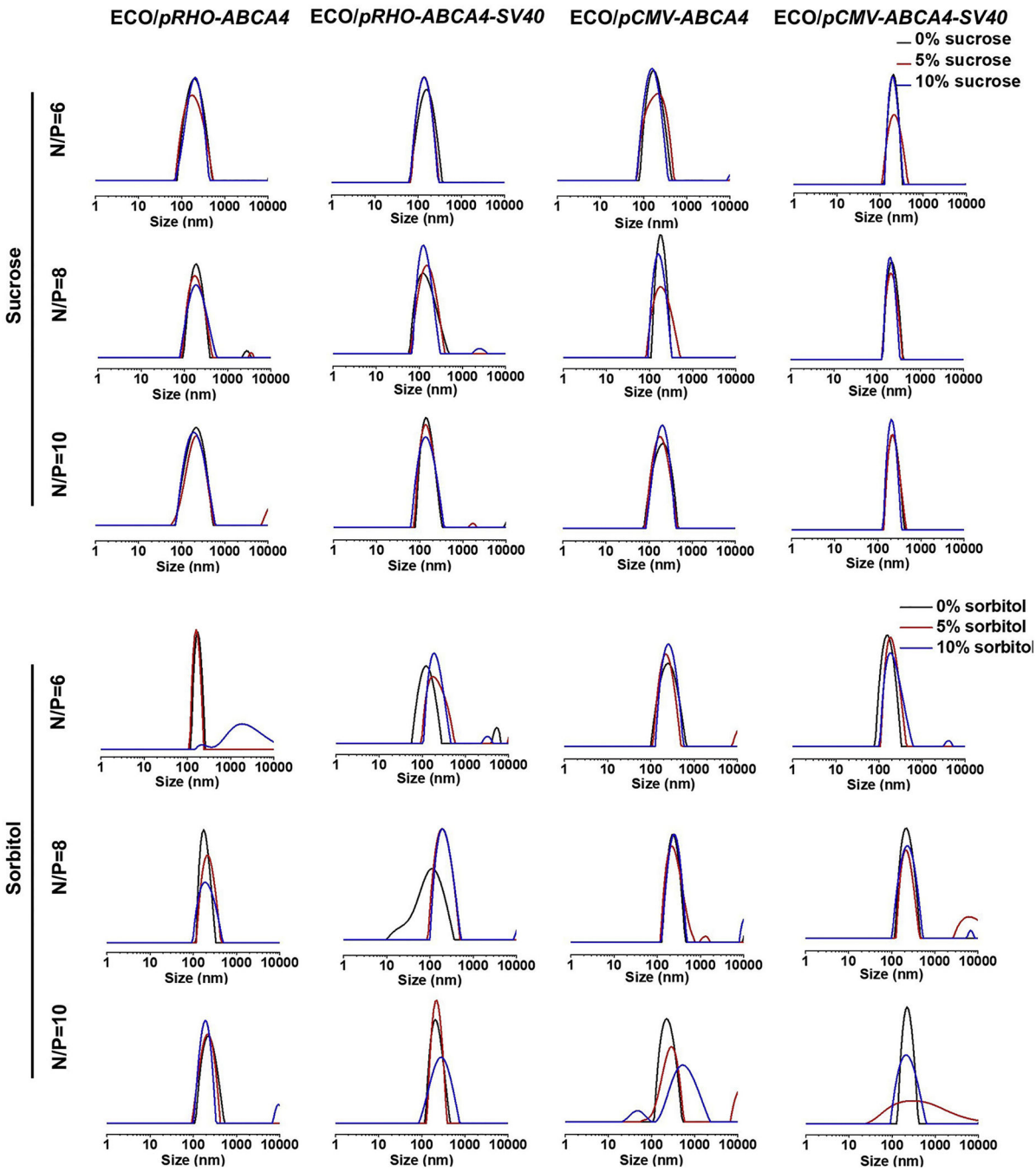

Fig. 2.

Size distributions of the nanoparticles of ECO with *pCMV–ABCA4, pCMV–ABCA4–SV40, pRHO–ABCA4*, and *pRHO–ABCA4–SV40* in the presence of sucrose and sorbitol as measured by dynamic light scattering.

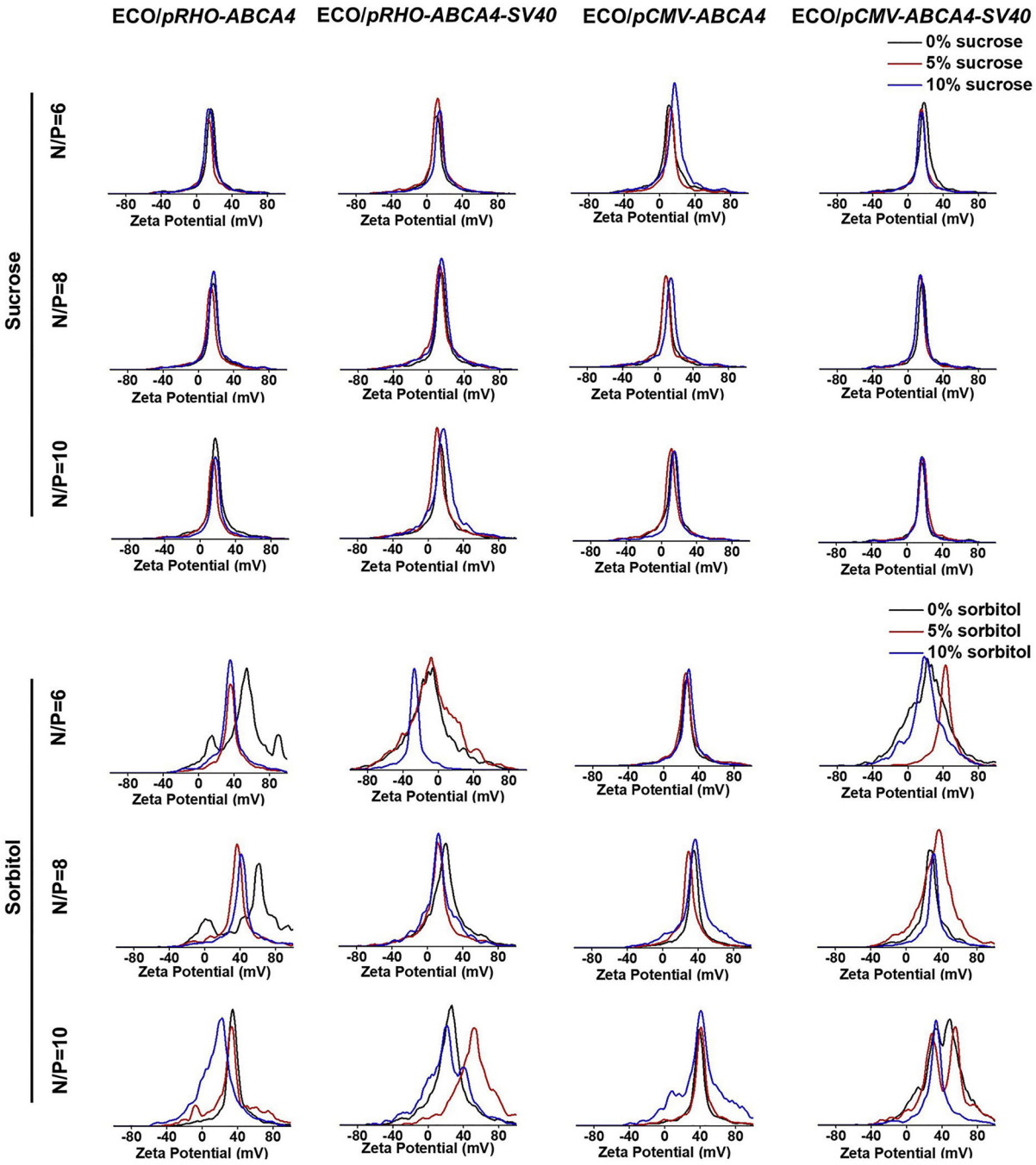

Fig. 3.

Zeta potential distributions of the nanoparticle formulations of ECO with *pCMV–ABCA4, pCMV–ABCA4–SV40, pRHO–ABCA4*, and *pRHO–ABCA4–SV40* in existence with sucrose and sorbitol as stabilizers.

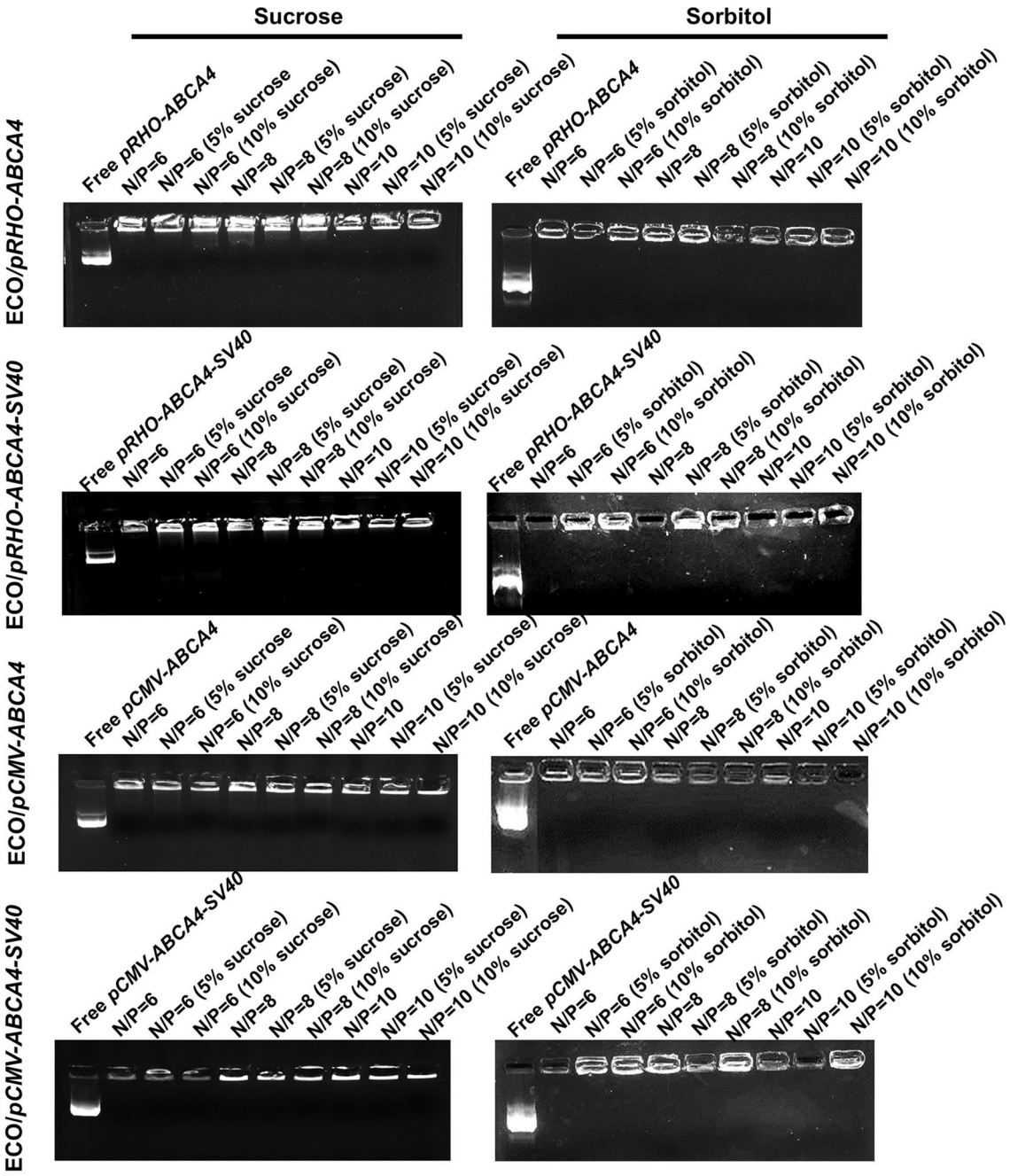

Fig. 4.

Agarose gel electrophoresis showing the encapsulation of plasmid DNA in the nanoparticles formulated by ECO with *pCMV–ABCA4, pCMV–ABCA4–SV40, pRHO–ABCA4*, and *pRHO–ABCA4–SV40* in the presence of sucrose and sorbitol.

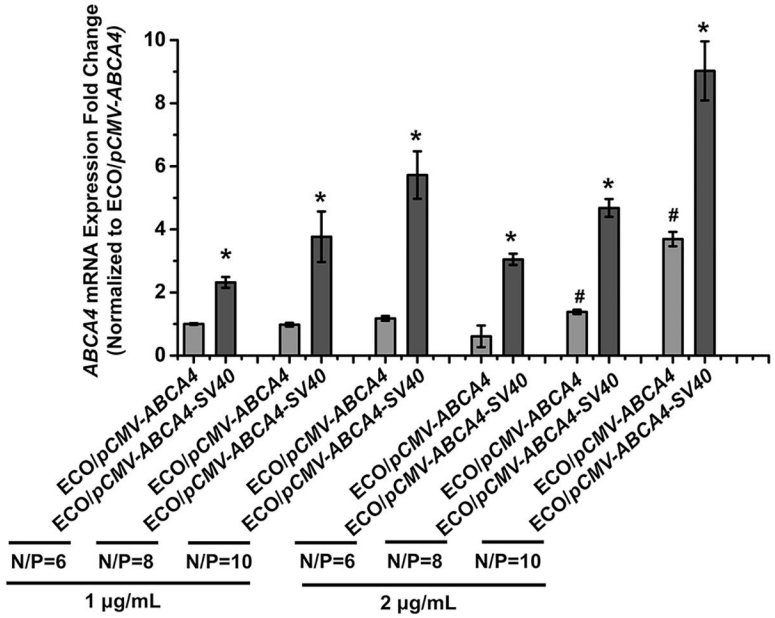

Fig. 5.

In vitro transfection of ECO/*pCMV–ABCA4* and ECO/*pCMV–ABCA4–SV40* nanoparticles in ARPE-19 cells demonstrated by qRT-PCR of *ABCA4* mRNA expression 48 h after transfections. *ABCA4* mRNA expressions were normalized to the expression of ECO/*pCMV–ABCA4* at N/P ratio of 6 and 1 μg/mL dose. (**p* < 0.05, relative to the mRNA expression of ECO/*pCMV–ABCA4* at the same condition. #p < 0.05, relative to the same nanoparticle formulation at 1 μg/mL.)

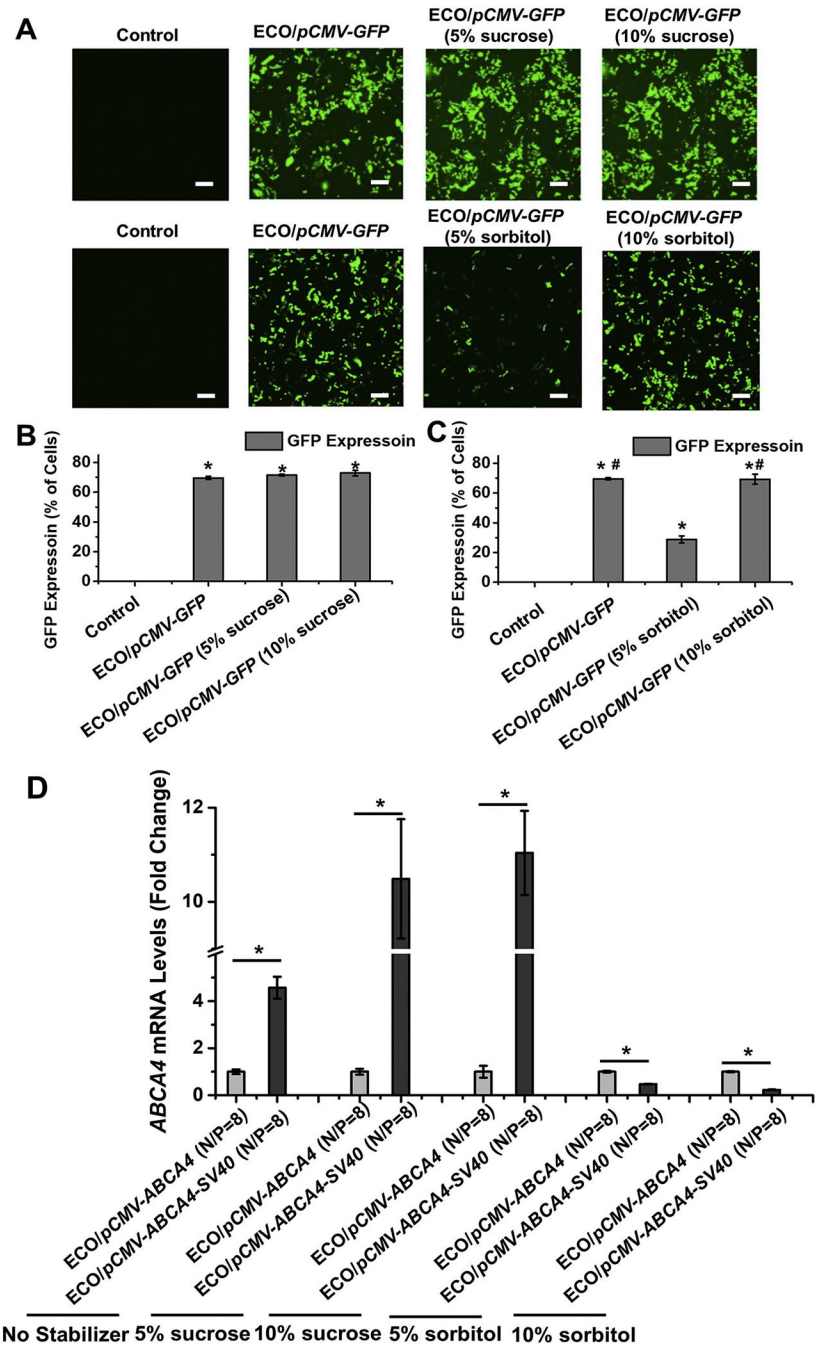

Fig. 6.

In vitro transfection of ECO/*pDNA* nanoparticles in ARPE-19 cells in the presence of sucrose or sorbitol. Confocal images (A) and flow cytometry (B, C) of GFP expression in ARPE-19 cells 48 h after transfection using ECO*/pCMV–GFP* nanoparticles (N/*P* = 8, DNA concentration of 1 μg/mL, under 0%, 5% and 10% sucrose or sorbitol). (D) *ABCA4* mRNA expression 48 h after transfections demonstrated by qRT-PCR using ECO/*pCMV–ABCA4* and ECO/*pCMV–ABCA4–SV40* nanoparticles (N/P ratios of 6, 8 and 10, DNA concentration of 1 μg/mL, under 0%, 5% and 10% sucrose or sorbitol). *ABCA4* mRNA

expressions of ECO/*pCMV–ABCA4–SV40* nanoparticles were normalized to those of ECO/*pCMV–ABCA4* nanoparticles. (Scale bars represent 20 μm. *$p < 0.05$, relative to the non-treated control in B and C. #p < 0.05, relative to the GFP expression in 5% sorbitol. *p < 0.05, between the two groups under the line in D).

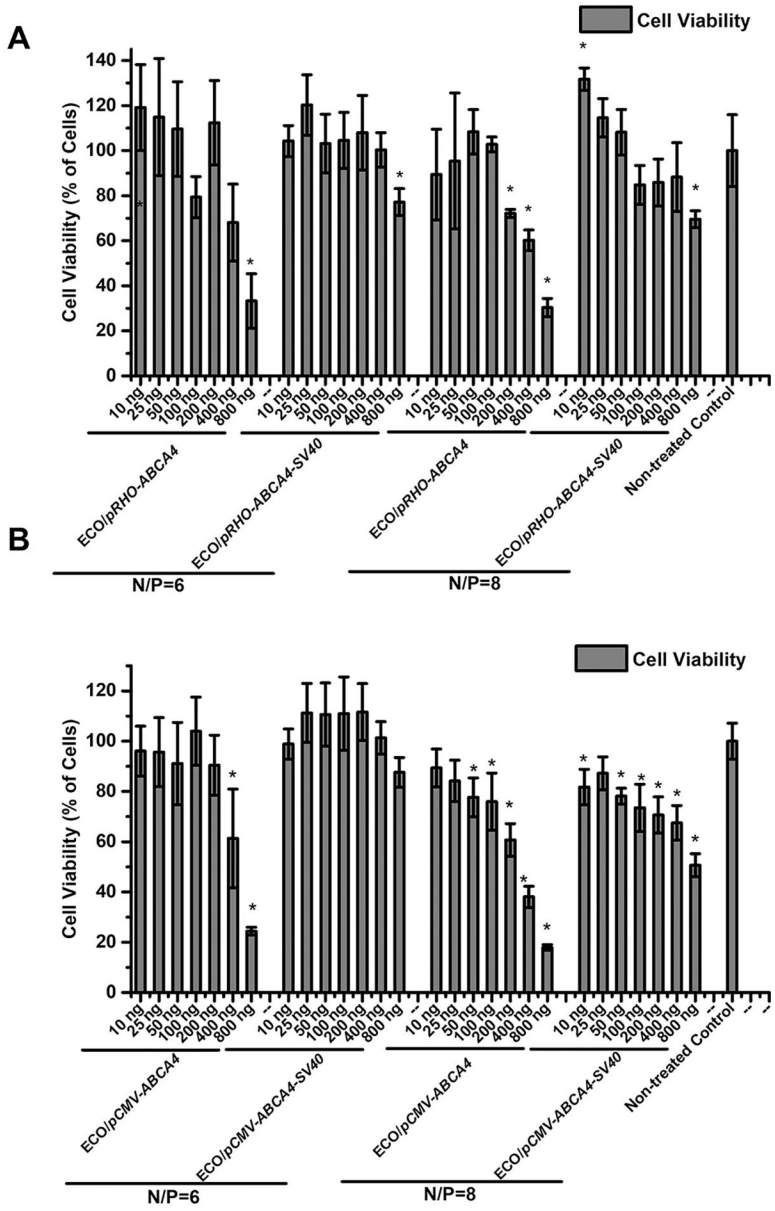

Fig. 7.

CCK-8 assay of cytotoxicity of (A) ECO/*pRHO–ABCA4,* ECO/*pRHO–ABCA4–SV40,* (B) ECO/*pCMV–ABCA4*, and ECO/*pCMV–ABCA4–SV40* nanoparticles in ARPE-19 cells 48 h after transfection (*$P < 0.05$ relative to non-treated control).

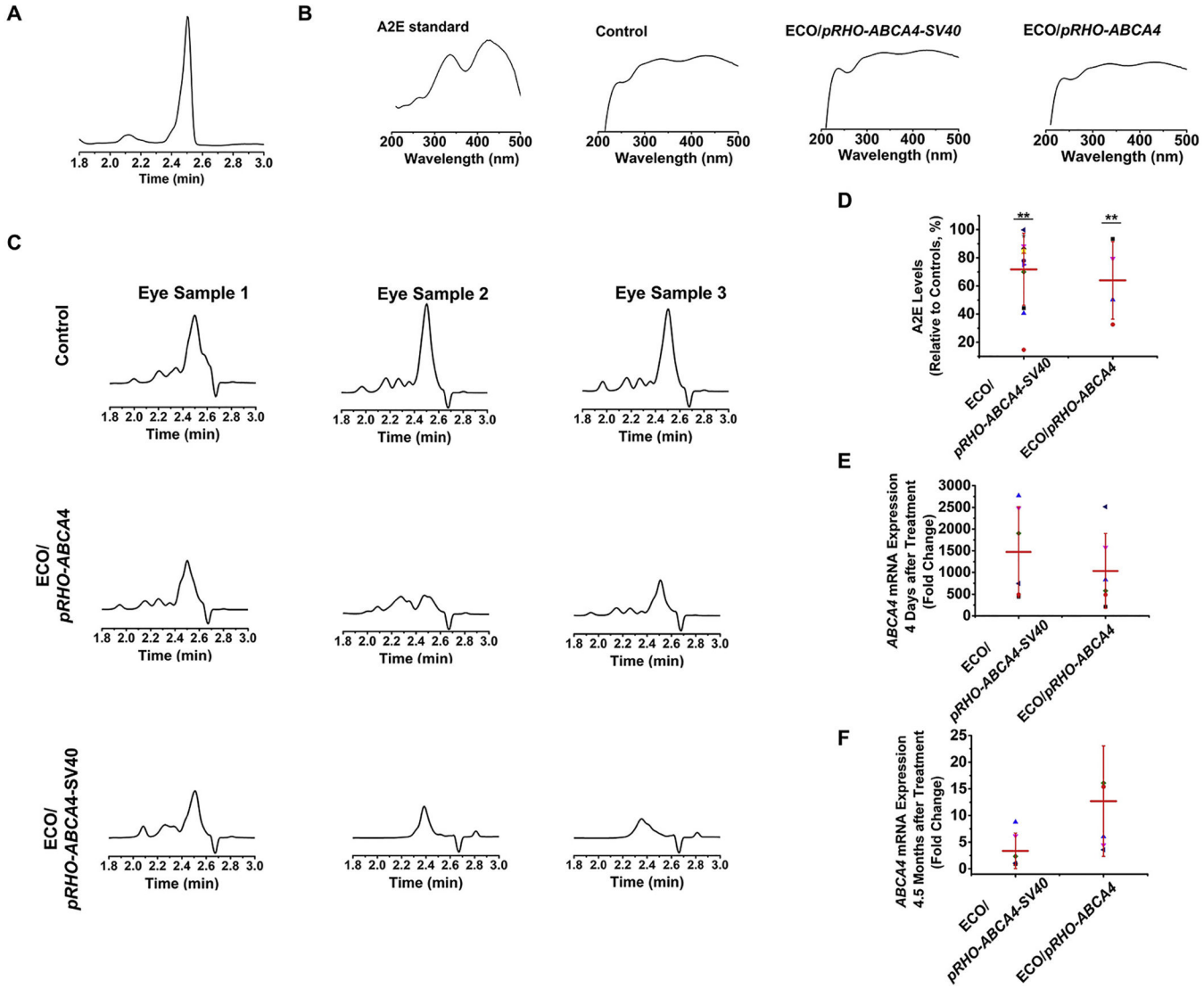

Fig. 8.

Efficacy of ECO/*pRHO–ABCA4* and ECO/*pRHO–ABCA40–SV40* nanoparticles for preventing A2E accumulation in *Abca4*$^{-/-}$ mice. (A) HPLC analysis of synthesized A2E standard. (B) A2E spectra of synthesized A2E standard, and samples from nanoparticle treated and control mice. (C) HPLC chromatograms of A2E from control, ECO/*pRHO–ABCA4,* and ECO/p*RHO–ABCA40–SV40* nanoparticles treated *Abca4*$^{-/-}$ mice 8 months after subretinal injections. (D) Quantitative A2E levels of ECO/*pRHO–ABCA4* and ECO/*pRHO–ABCA40–SV40* nanoparticles treated *Abca4*$^{-/-}$ mice relative to PBS control mice 8 months after subretinal injections. *ABCA4* mRNA expression (E) 4 days and (F) 4.5 months after subretinal treatments of ECO/*pRHO–ABCA4* and ECO/*pRHO–ABCA4–SV40* nanoparticles in *Abca4*$^{-/-}$ mice. (error bars = ± SD, $^{**}P < 0.05$ relative to control eyes. Statistical analysis was conducted with one-way ANOVA).